POLITECNICO DI TORINO
Repository ISTITUZIONALE

Low temperature tempering of low alloy 39NiCrMo3 and 36NiCrMo16 quenched and tempered steels

Original
Low temperature tempering of low alloy 39NiCrMo3 and 36NiCrMo16 quenched and tempered steels / Firrao, D., Matteis, P., De Sario, A.. - In: MATERIAL DESIGN & PROCESSING COMMUNICATIONS. - ISSN 2577-6576. - 3:1(2021). [10.1002/mdp2.142]

Availability:
This version is available at: 11583/2784709 since: 2021-02-11T13:07:09Z

Publisher:
Wiley

Published
DOI:10.1002/mdp2.142

Terms of use:

This article is made available under terms and conditions as specified in the corresponding bibliographic description in the repository

Publisher copyright

(Article begins on next page)

27 November 2026

Low temperature tempering of low alloy 39NiCrMo3 and 36NiCrMo16 quenched and tempered steels

D. Firrao[a], P. Matteis[b,*], A. De Sario[c]

[a] Formerly with Politecnico di Torino, Corso Duca degli Abruzzi 24, Torino, It-10129, Italy

[b] Politecnico di Torino, Corso Duca degli Abruzzi 24, Torino, It-10129, Italy

[c] Vimi Fasteners S.p.A., Via Labriola 19, Novellara, It-42017, Italy

* Corresponding author; e-mail address: paolo.matteis@polito.it

Abstract

It is well known that quenched and tempered alloy steel components with ultimate tensile strength in excess of 1400 MPa are seldom employed as mechanical components, due to their not adequate ductility, as ascertained by multiple researches performed during World War II and soon after. Nevertheless, use of low temperature tempered steels in some niche applications, as well as researches performed on surface heat treated high carbon steels and on their behavior upon tempering in the vicinity of 200°C have stemmed into renewed interest in quenched and low temperature tempered low alloy steels. Application to EN 39NiCrMo3 and EN 36NiCrMo16 steel bars is examined here, by means of tensile and hardness tests and fractographic and metallographic examinations after quenching and tempering in the 160 to 440 °C temperature range.

Running title: Low temperature tempering of low alloy steel

Keywords: High strength steels, low temperature tempering, low alloy steels

Conflict of interest: the authors have no conflict of interest.

Low temperature tempering of low alloy 39NiCrMo3 and 36NiCrMo16 quenched and tempered steels

Abstract

It is well known that quenched and tempered alloy steel components with ultimate tensile strength in excess of 1400 MPa are seldom employed as mechanical components, due to their not adequate ductility, as ascertained by multiple researches performed during World War II and soon after. Nevertheless, use of low temperature tempered steels in some niche applications, as well as researches performed on surface heat treated high carbon steels and on their behavior upon tempering in the vicinity of 200°C have stemmed into renewed interest in quenched and low temperature tempered low alloy steels. Application to EN 39NiCrMo3 and EN 36NiCrMo16 steel bars is examined here, by means of tensile and hardness tests and fractographic and metallographic examinations after quenching and tempering in the 160 to 440 °C temperature range.

Keywords

High strength steels, low temperature tempering, low alloy steels

1. Introduction

Researches published in USA just after World War II on low alloy quenched and tempered steels have shed a negative light on the use of low alloyed steels in the medium to low temperature tempering regime, where they reach UTS values well above 1400 MPa (Sachs et al., 1950) which was since then considered for a long time the limiting safe tensile strength in mechanical apparatuses.

For example, according to the ISO 898 international standard, quenched and tempered steel bolts must be tempered at temperatures not lower than 425 °C.

There have been, however, several niche application of quenched and low-temperature tempered steels, especially for wear resistance (Dudzinski et al, 2008), armor (Borvik et al., 2009), and car safety (Karbasian and Tekkaya, 2010).

Better assessment of stress and strain distribution in joining steel components and the everlasting quest for higher and higher strengths to reduce mass in critical applications, urge revisiting the whole field of medium to low tempering temperatures to set not too a daring UTS limit to be used by mechanical engineers in their new designs.

In such range of tempering temperatures, quenched steel microstructures change, as mainly studied by M. Cohen and his co-workers at MIT (Averbach and Cohen, 1949, Roberts et al., 1953, Mentser, 1959,

Cohen, 1983), yielding cubic martensite (0.3% C) and ε-carbides - now termed conversion carbides (Krauss, 1984, Lee and Krauss 1992).

Tests performed by the senior author while investigating induction hardening and low temperature tempering of UNI 88MnV8KU tool steel (similar to ISO 90MnCrV8) constitute the starting point of a new research program aiming to fully assess a safe use of ultra high strength steels.

In the case of 88MnV8KU steel, a peaking of impact resistance was ascertained at 210 °C tempering temperature, with only a reasonably low loss of hardness in respect to the as quenched steel (figure 1).

The use of a steel more suitable for mechanical apparatuses has induced the authors in 2015 to repeat low tempering tests on two different medium carbon, low alloy Ni-Cr-Mo quenched and tempered steel grades, namely 39NiCrMo3 and 36NiCrMo16 (compliant to the then existing EN 10083 European standard), where the use of a high Ni content should counteract the low ductility imparted by the presence of cubic martensite in the steel microstructure.

2. Experiments

The two steels were received as 20 mm diameter rods in the spheroidized annealed metallurgical state, with the elemental composition given in table I.

Cylindrical specimens with 11 or 17 mm diameter were machined from the bars and heat treated, with the following steps: cleaning; austenitizing at 900 °C for 60 min; quenching in agitated oil at 60 °C; cleaning; tempering for 60 min at different temperatures in the 160 to 440 °C range.

The heat treated specimens were characterized by means of optical metallography, X-ray diffraction and hardness and tensile testing.

Several tensile samples were tested for each condition, with 9 or 10 mm calibrated diameter and proportional gage length (equal to 5 times the diameter).

In particular, 2 tensile specimens with 10 mm diameter and one tensile specimen with 9 mm diameter were tested for each examined steel grade and for each of the following tempering temperatures: 220, 240, 320, 400 and 420 °C; furthermore, at least 10 tensile specimens fabricated with the 36NiCrMo16 steel grade, with 10 mm diameter, were tested for each of the following tempering temperatures: 160, 180, 200 and 440 °C.

In most cases, the yield stress was measured qualitatively on the test autographic record, causing a relatively large scatter and uncertainty.

Finally, representative broken tensile specimens were subjected to fractographic analysis by means of electron microscopy and energy dispersion spectroscopy.

3. Results

3.1 Microstructures

The steel microstructure after quenching was fully martensitic (with slight chemical segregation in the 36NiCrMo16 steel case, figure 2a); its evolution upon tempering is shown in figures. 2 for steel 36NiCrMo16 and similar microstructures for steel 39NiCrMo3 are displayed in figure 3.

Microstructure variations are not evident in the optical microscopy examinations up to the 200 °C tempering temperature (see Fig. 2a to c for the 36NiCrMo6 steel); in contrast, after tempering at 440 °C, in the 36NiCrMo16 case, shown in Fig. 2d, microstructural features become sharper and the evolution from a martensitic structure to a mixture of ferrite and spheroidal cementite is evident.

The light microscopy examination also allowed to detect a microstructural evolution in the 39NiCrMo3 steel above 220 °C tempering temperature (figure 3). Moreover, more detailed examination by SEM (figures 3b and d) shows that, by tempering at increasing temperatures, fine transition carbide precipitation has already begun during tempering at 220 °C; precipitation of larger Fe_3C carbides starts during tempering at 240 °C, and coalescence of Fe_3C carbides starts during tempering at 320 °C.

Finally, X-ray diffraction analyses performed on the 39NiCrMo3 steel grade allowed to detect traces of retained austenite after quenching and tempering at 220 °C, but not after tempering at 240 °C or more; thus confirming the transformation of retained austenite upon tempering at 240 °C or more.

3.2 Mechanical properties

The mechanical properties at room temperature, as a function of the tested tempering temperature, are illustrated in figure 4 (tensile strength) and 5 (ductility).

The quenched and tempered 36NiCrMo16 steel grade exhibits its maximum Ultimate Tensile Strength (UTS) after tempering at about 180 °C. By increasing the tempering temperature above 200 °C, for both steels, the UTS show a marked decrease tendency. However, the 39NiCrMo3 steel grade exhibits a slightly higher UTS at 220 °C, and then a slightly steeper decline, in respect to the 36NiCrMo16 one.

The trend of the yield stress is similar to that of the UTS, except that, for the 36NiCrMo16 steel grade, the peak value is closer to 240 °C.

In contrast, the ductility (or elongation at fracture) and the reduction of area at fracture increase steeply with the tempering temperature below 220 °C (at least for the 36NiCrMo16), and thereafter exhibit only smaller variations up to the higher examined tempering temperature (440 °C). The ductility and the reduction of area are also similar for the two steels, with the 39NiCrMo3 exhibiting only slightly lower values.

3.3 Fractography

The tensile fracture surface of both steels after tempering at the examined temperatures always exhibits the well known cup-and-cone morphology, figures 6 (steel 39NiCrMo3) and 7 (steel 36NiCrMo16).
Figure 7 allows to appreciate that the conical region becomes larger by increasing the tempering temperature up to about 200 - 220 °C, and is thereafter nearly constant in size.
The microscopic fracture mechanism in the same conical region does not change, always exhibiting shallow and oriented dimples, formed by ductile shear plastic instability.
In the central region (figures from 8 to 14) the prevalent fracture mode is always ductile microvoid coalescence. At tempering temperatures equal to or lower than 200 °C, which were examined only in the 36NiCrMo16 steel case, the central region exhibits shallow and homogeneous dimples confined on a flat and smooth fracture plane (figure 8a); by increasing the tempering temperature, these gradually evolve towards deeper and less homogeneous dimples (figures 9 and 10); a much rougher overall surface was eventually observed in both steels when the tempering temperature was 220 °C or more (figures from 11 to 14)
The fracture surfaces formed after low temperature tempering at 160 °C in the 36NiCrMo16 steel also exhibit in their central region secondary cracks (figure 8b) and large brittle islands (figure 8c and d); by increasing the tempering temperature at and above 180 °C, secondary cracks do not occur anymore, but several small and large brittle islands occur after tempering at 180 and 200 °C, mostly lying above or below the mean fracture plane and thus resulting in a more complex fracture path (figures 9a and 10a). None of these features occurs after tempering in the 220 to 440 °C range, neither in the 36NiCrMo16 steel (figure 12 and 14), nor in the 39NiCrMo3 one (figures 11 and 13).
The fracture mechanism close to the secondary cracks and inside the brittle islands (as examined in the 36NiCrMo16 case) is mostly intergranular after tempering at 160 °C (figure 8b, d), it is quasi-cleavage after tempering at 200 °C (figure 10), and it is mixed (intergranular and cleavage) after tempering at 180 °C. The brittle islands seem to irradiate from point defects, which may be strings of submicrometric inclusions causing first a small crack, then a blunting region, and finally the whole brittle islands (figures 8c and 10b). Only in one instance a large spherical inclusion, with about 40 µm diameter, consisting of aluminum, calcium and magnesium oxides, was detected on the fracture surface (figure 10c, d).

4. Conclusions

Preliminary results of a research program aiming at the safe employment of conventional medium carbon, low alloy steels in the low tempering temperature regime indicate that, by oil quenching and tempering in the 220 - 320°C interval, UTS well above 1700 MPa can be achieved, with 10% elongation-to-fracture, and fully ductile fracture surfaces. By tempering below 240°C, UTS above 1800

MPa and YS above 1600 MPa are achieved. Therefore, a 30% increase over the conventional 1400 MPa limit can be safely achieved.

In the same 220 - 320°C tempering range, the steel microstructure exhibits a significant variation with the progressive disappearance of retained austenite and the increasing appearance of transition carbides and cementite carbides. The latter carbides are already coalescing during tempering at 320°C. Conflicting embrittling and toughening phenomena conjure to keep the elongation-to-fracture practically constant at 10% in this tempering range.

The here reported tensile test results are overall compatible with data pertaining to another quenched and tempered Ni-Cr-Mo steel (AISI 4340) (Spretnak and Firrao, 1980; Firrao et al., 1984).

In particular, the here reported tensile test results, for both examined steels, do not highlight evident signs of temper embrittlement. In one of the examined steels (EN 36NiCrMo16), this fact may have been favored by a slightly higher than usual Mo content (0.28%); however, this was not the case for the other examined steel (EN 39NiCrMo3). Therefore, it may be hypothesized that the absence of temper embrittlement was promoted by the relatively short heat treating times, which were possible because the specimens were relatively small, and may not have allowed enough time for the grain boundary segregation of harmful elements.

The origin of the brittle zones on the fracture surfaces, after tempering at 180 and 200 °C, must be further investigated.

References

Averbach B.L., Cohen M., 1949, The isothermal decomposition of martensite and retained austenite, Transactions of the American Society for Metals, vol. 41, 1024-1060.

Borvik T., Dey S., Clausen A.H., 2009, Perforation resistance of five different high-strength steel plates subjected to small-arms projectiles, International Journal of Impact Engineering, vol. 36(7), 948-964.

Cohen M., 1983, Opening of the Peter G. Winchell symposium on the tempering of steel, Metallurgical and Materials Transactions A, vol. 14, 991-993.

Dudzinski, W., Konat L., Pekalski G., 2008, Structural and strength characteristics of wear-resistant martensitic steels, Archives of Foundry Engineering, vol. 8(2), 21-26.

EN 10083-3. Steels for quenching and tempering. Part 3: Technical delivery conditions for alloy steels. European Committee for Standardization, Brussels, Belgium, 2006.

Firrao D., Roberti R., De Benedetti B., 1984, Riflessi del trattamento di austenitizzazione sulla tenacità a frattura dell'acciaio AISI 4340 bonificato, Industria Meccanica, vol. 36, 641-644.

ISO 898-1: Mechanical properties of fasteners made of carbon steel and alloy steel. Part 1: Bolts,

screws and studs with specified property classes - Coarse thread and fine pitch thread. International Organization for Standardization, Geneva, Switzerland, 2013.

Karbasian, H., Tekkaya, A.E., 2010), A review on hot stamping, Journal of Materials Processing Technology, vol. 210(15), 2103-2118.

Krauss G., 1984, Tempering and structural changes in ferrous martensitic structures, in: Marder A.R., Goldstein J.J. (editors), Phase Transformations in Ferrous Alloys, TMS-AIME, Warrendale, PA, USA, 101-123.

Lee H.C., Krauss G., 1992, Intralath carbide transition in martensitic medium-carbon steels tempered between 200 and 300 °C, in: Fundamentals of Aging and Tempering in Bainitic and Martensitic Steel Products, ISS, Warrendale, PA, USA, 39-43

Mentser M., 1959, Magnetic analysis of phase changes produced in tempering a high carbon steel, Transactions of the American Society for Metals, vol. 51, 517.

Roberts C.S., Averbach B.L., Cohen M., 1953, The mechanism and kinetics of the first stage of tempering, Transactions of the American Society for Metals, vol. 45, 576-604.

Sachs G., Sangdahl G.S., Brown W.F., 1950, New notes on high strength heat-treated steels, Iron Age, Nov. 23, 59-63, and Nov. 30, 76-80.

Spretnak J.W., Firrao D., 1980, Considerazioni sul ruolo dell'instabilità plastica nella formazione di fratture di tipo duttile, Metallurgia Italiana, vol. 72, 525-534.

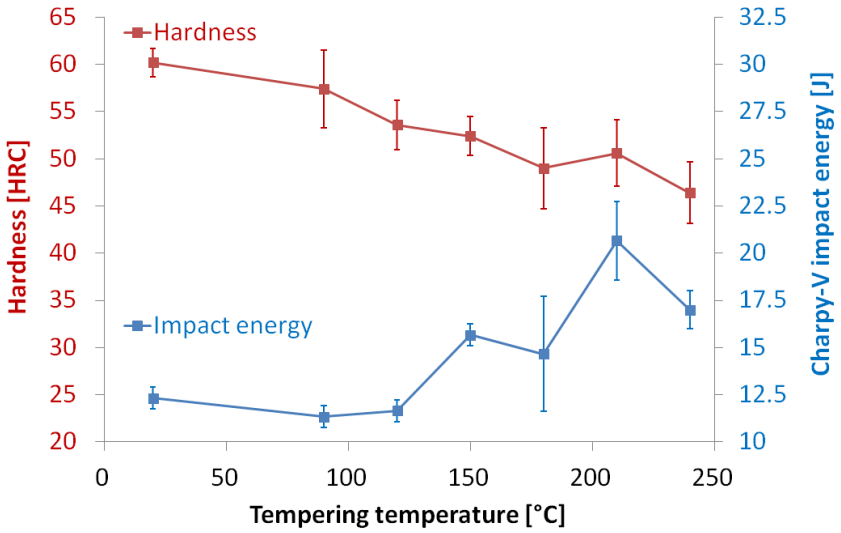

Fig. 1 – Impact energy and hardness of quenched and tempered 88MnV8KU tool steel.

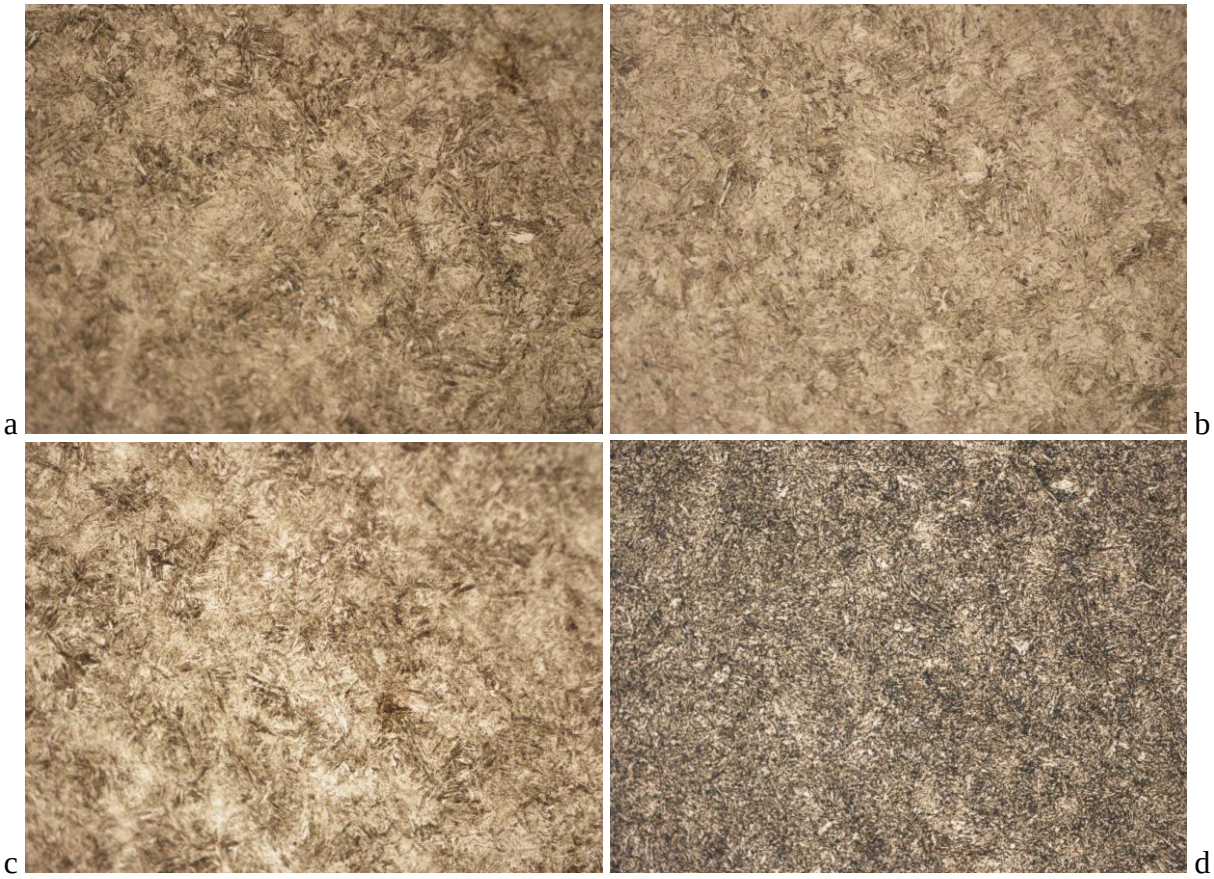

Fig. 2 – Steel 36NiCrMo16. Microstructure after quenching (a) and after tempering at 160 °C (b), 200 °C (c), and 440 °C (d). Optical microscopy after Nital etching. Original magnification: 500 x (actual size ≈ 100 x 75 μm).

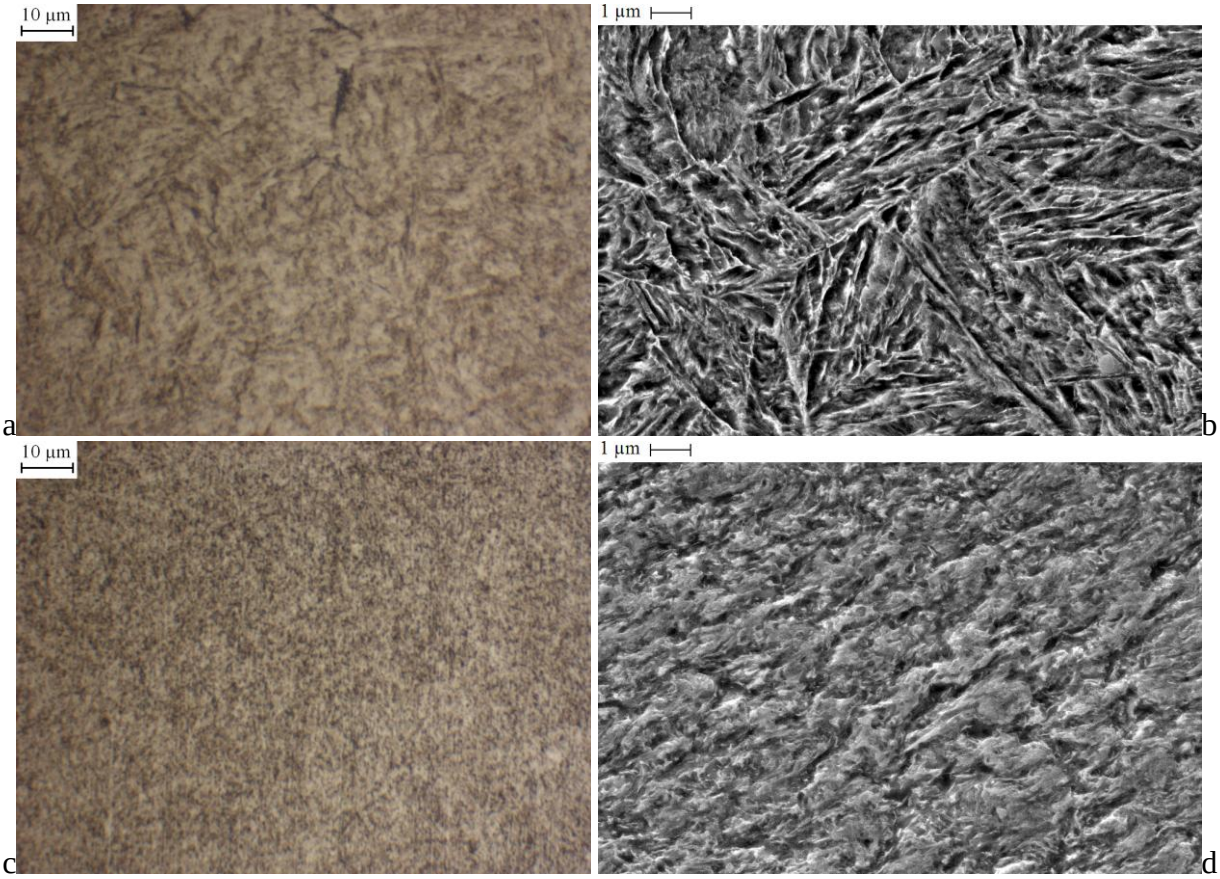

Fig. 3 – Steel 39NiCrMo3. Microstructure after quenching and after tempering at 220 °C (a, b) and 320 °C (c, d). Light microscopy (a, c) and electron microscopy (b, d).

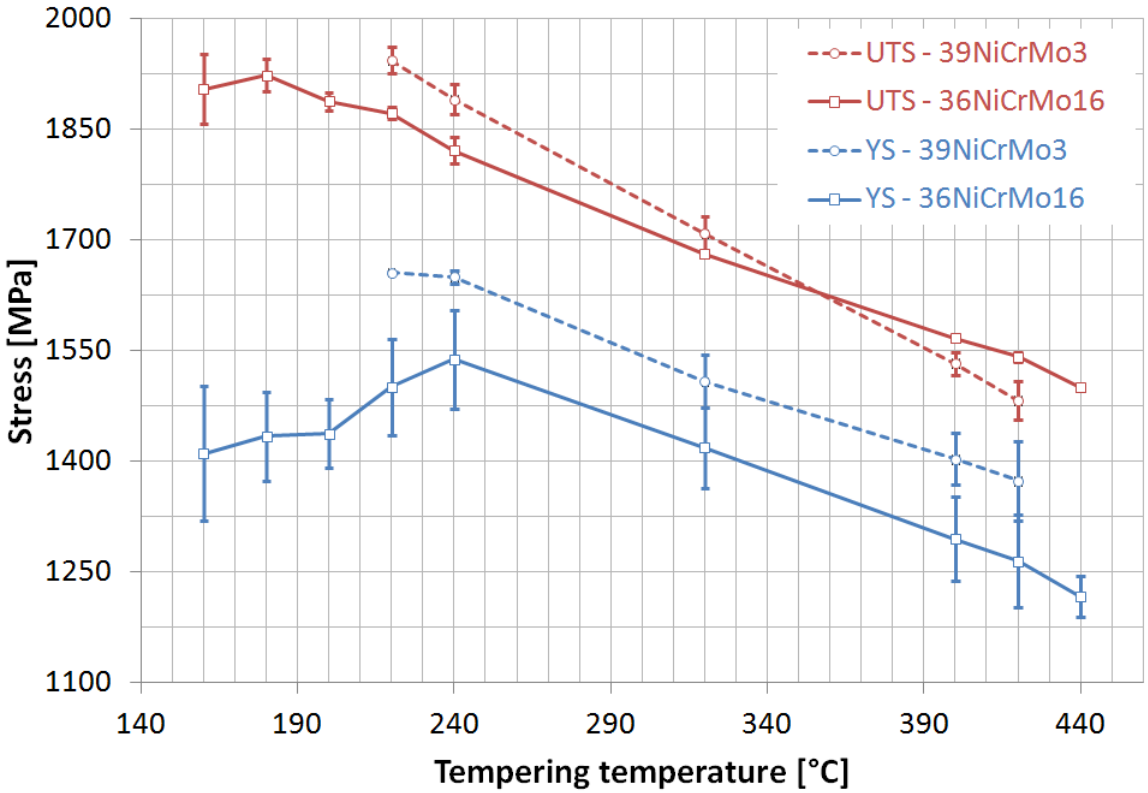

Fig. 4 – Yield Stress (YS) and Ultimate Tensile Strength (UTS) of the 39NiCrMo3 and 36NiCrMo16 steels as a function of the tempering temperature. All data points are mean values and the vertical bars represent the standard deviation.

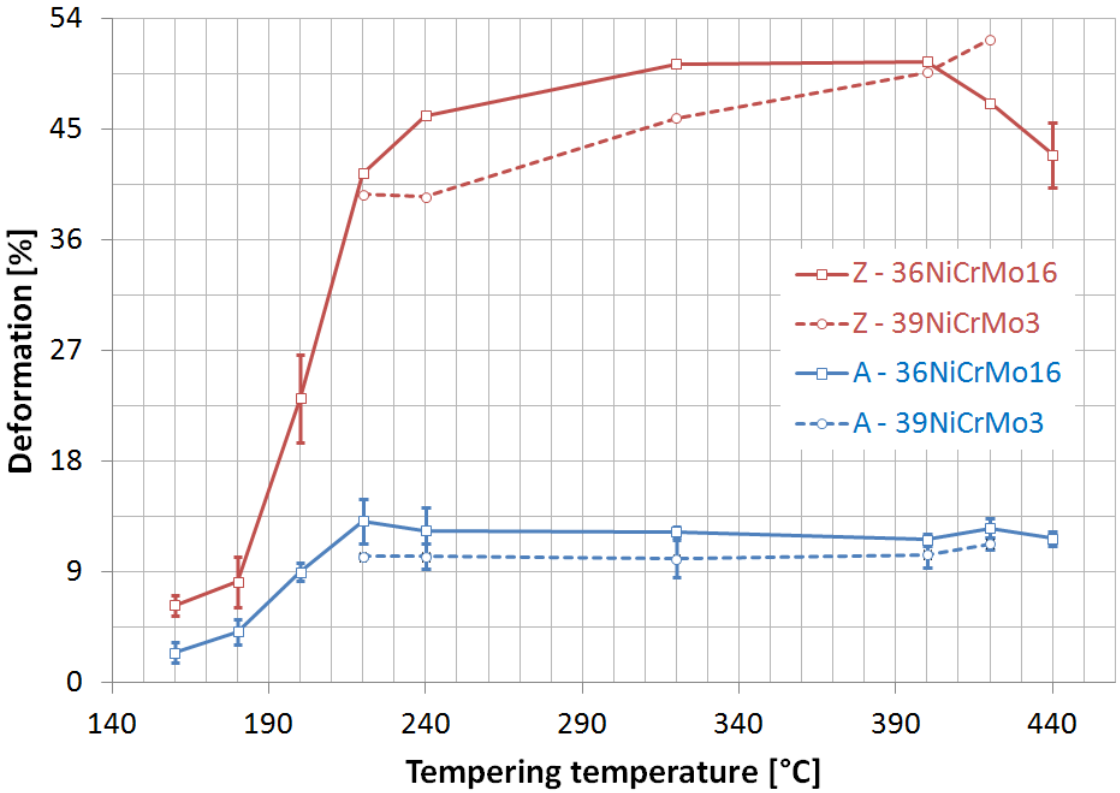

Fig. 5 – Elongation at fracture (A) and reduction of area (Z) of the 39NiCrMo3 and 36NiCrMo16 steels as a function of the tempering temperature. The Z data points between 220 and 420 °C are individual test results; all other data points are mean values. Vertical bars represent the standard deviation.

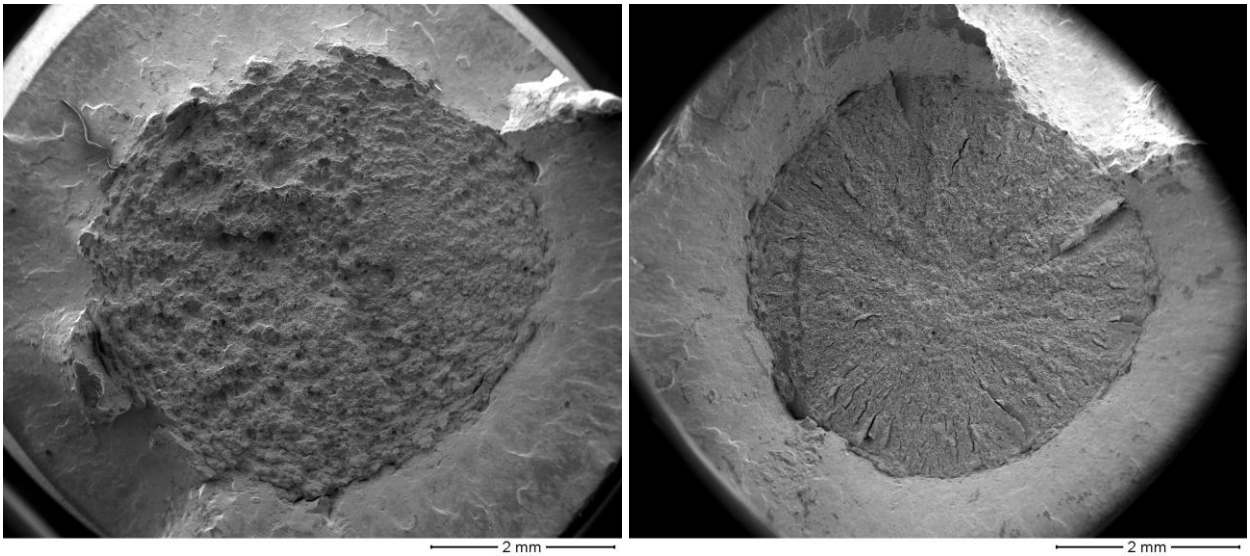

a b

Fig. 6 – Fracture surfaces of 39NiCrMo3 steel tensile specimens tempered at 240 °C (a) and 420 °C (b). Low magnification electron microscopy.

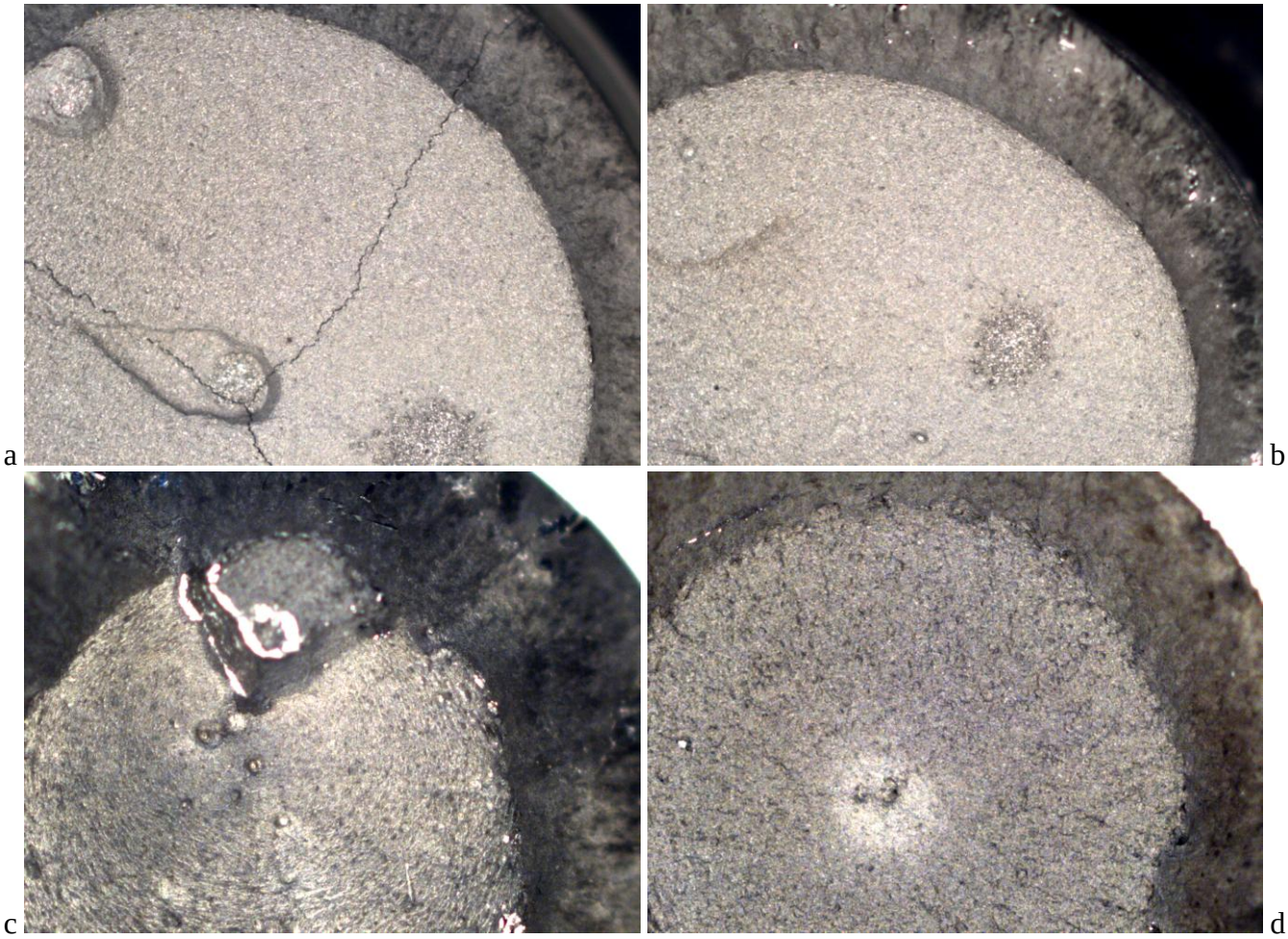

Fig. 7 – Fracture surfaces of 36NiCrMo16 steel tensile specimens tempered at 160 °C (a), 180 °C (b), 200 °C (c) and 440 °C (d). Low magnification optical microscopy. The initial diameter of the tensile specimens was 10 mm.

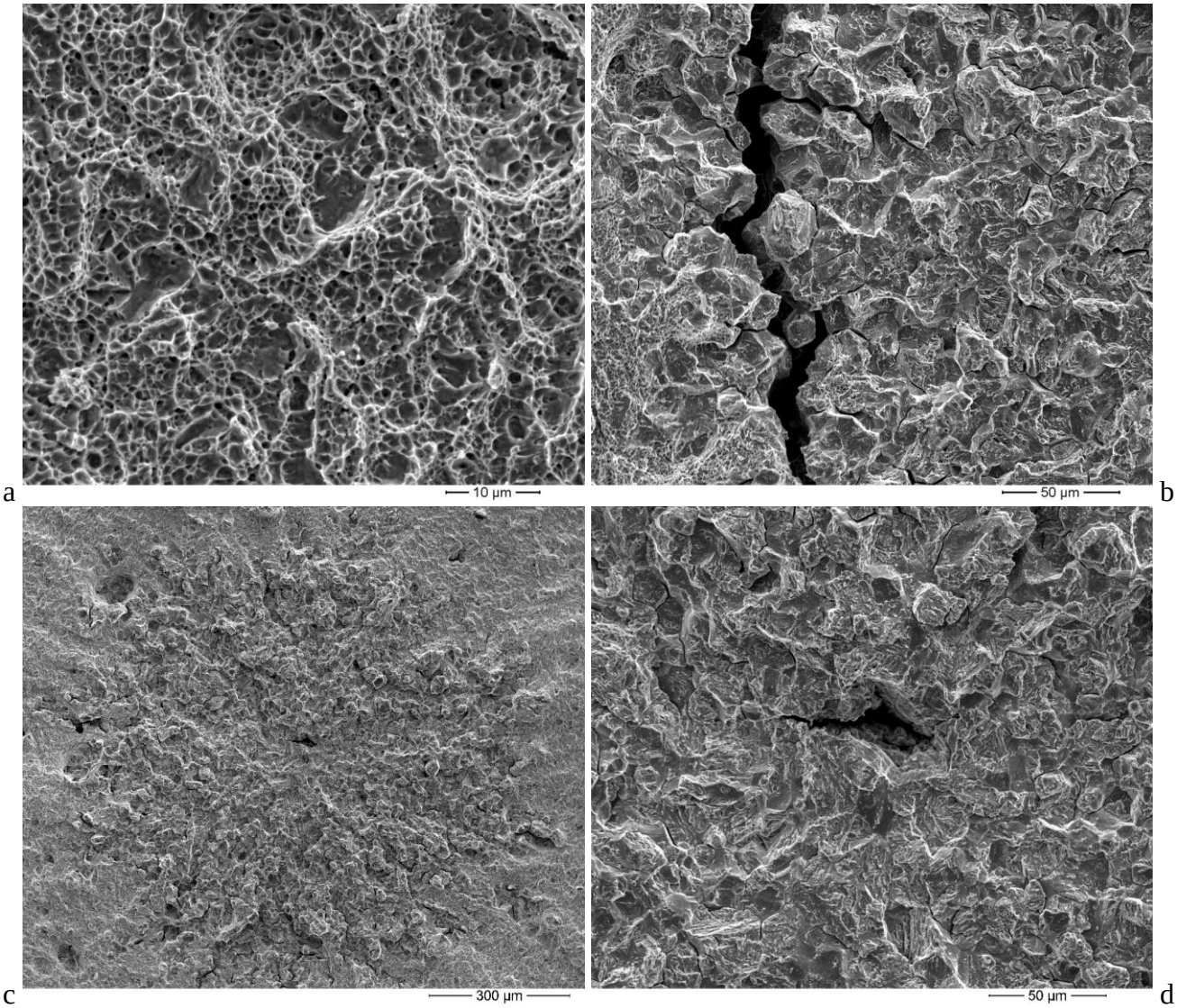

Fig. 8 – Fracture surface of a 36NiCrMo16 steel tensile specimen tempered at 160 °C. Electron microscopy. Central (normal) part. Prevalent ductile fracture mechanism (a); secondary crack (b); brittle fracture island (c, d).

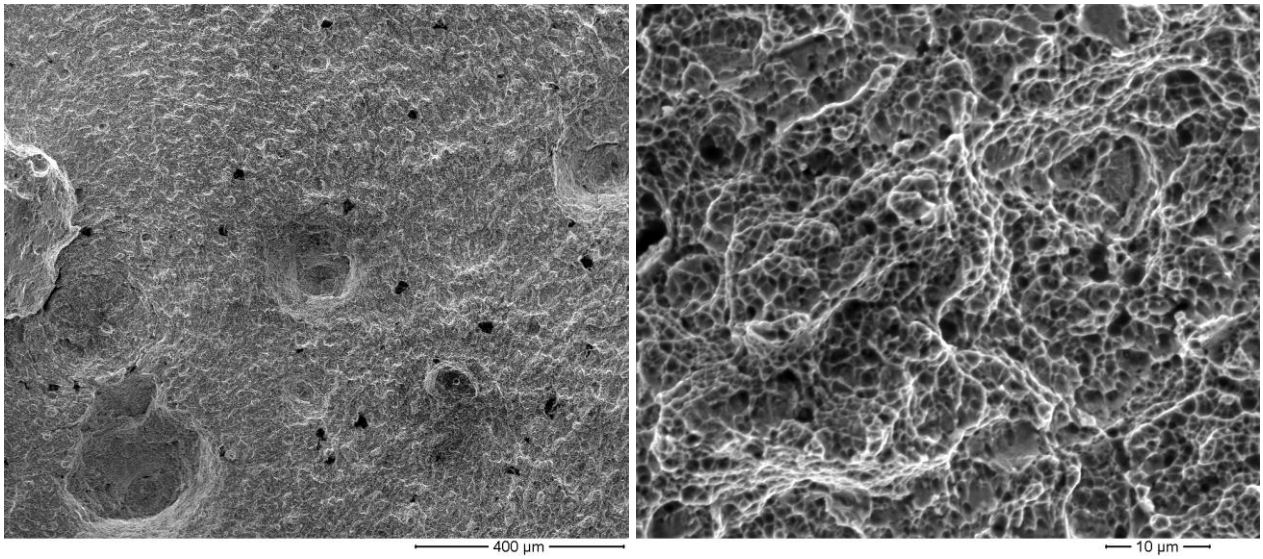

a b

Fig. 9 – Fracture surface of a 36NiCrMo16 steel tensile specimen tempered at 200 °C . Electron microscopy. Central (normal) part. Ductile fracture (prevalent) with brittle islands (a); detail of ductile fracture area (b).

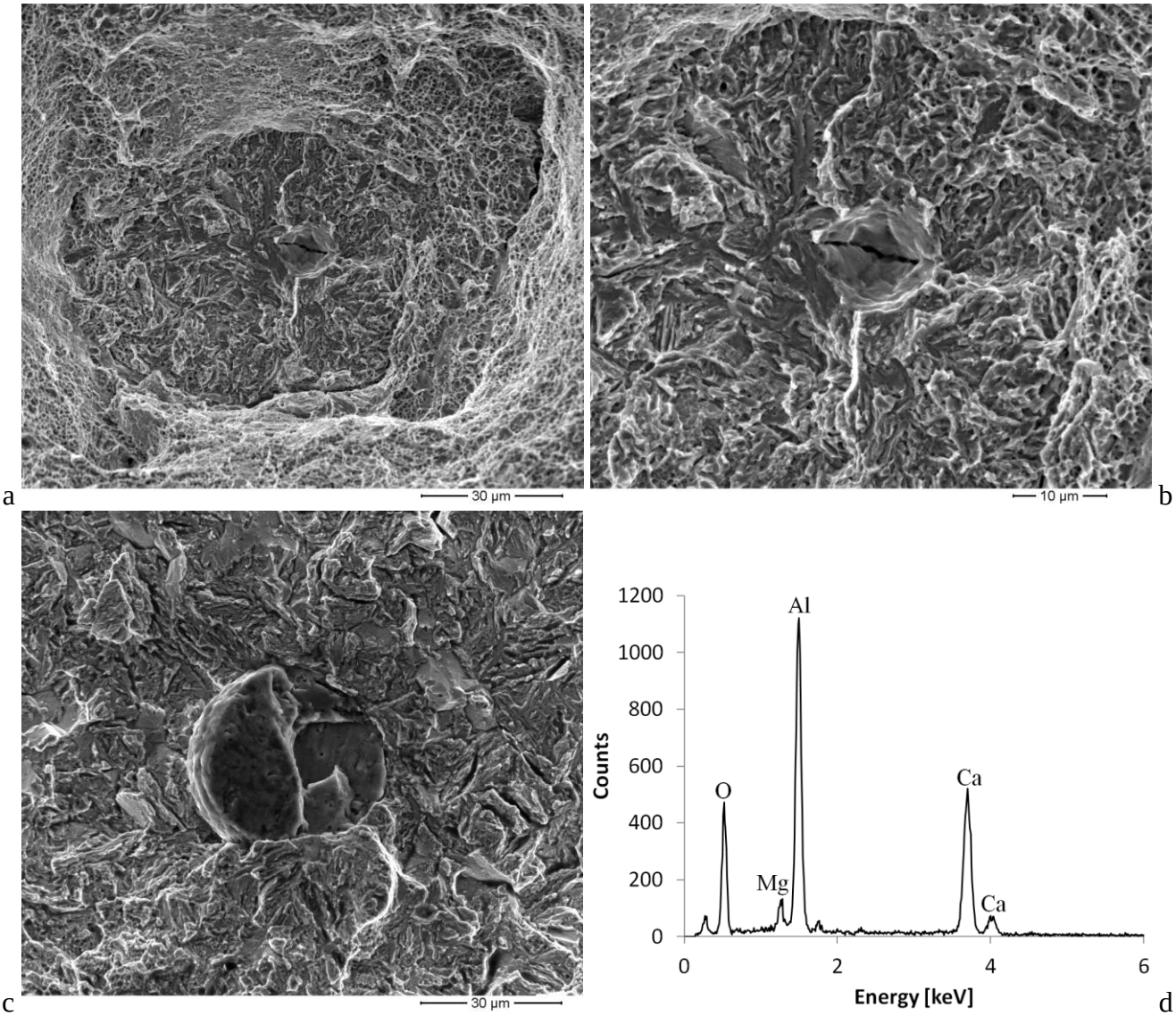

Fig. 10 – Fracture surface of a 36NiCrMo16 steel tensile specimen tempered at 200 °C. Electron microscopy. Central (normal) part. Brittle fracture island (a, b); brittle fracture around a large oxide inclusion (c) and Energy Dispersion Spectroscopy (EDS) analysis of the same inclusion (d).

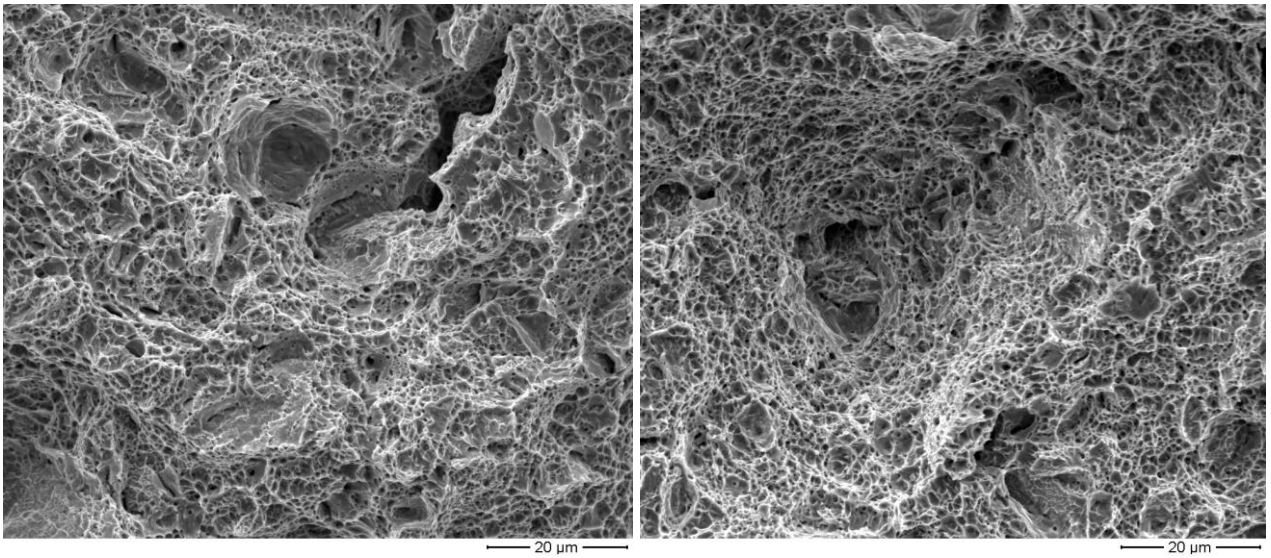

a b

Fig. 11 – Fracture surface of 39NiCrMo3 steel tensile specimens tempered at 220 °C (a) and 240 °C (b). Electron microscopy. Central (normal) part.

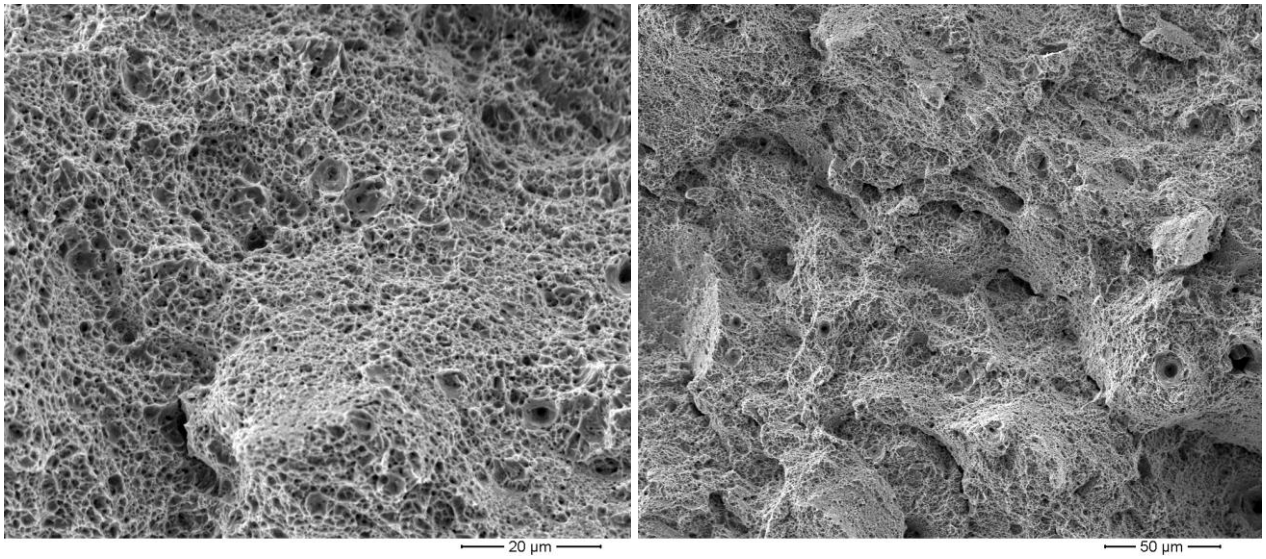

a b

Fig. 12 – Fracture surface of a 36NiCrMo16 steel tensile specimen tempered at 320 °C. Electron microscopy. Central (normal) part. Ductile fracture (a, b).

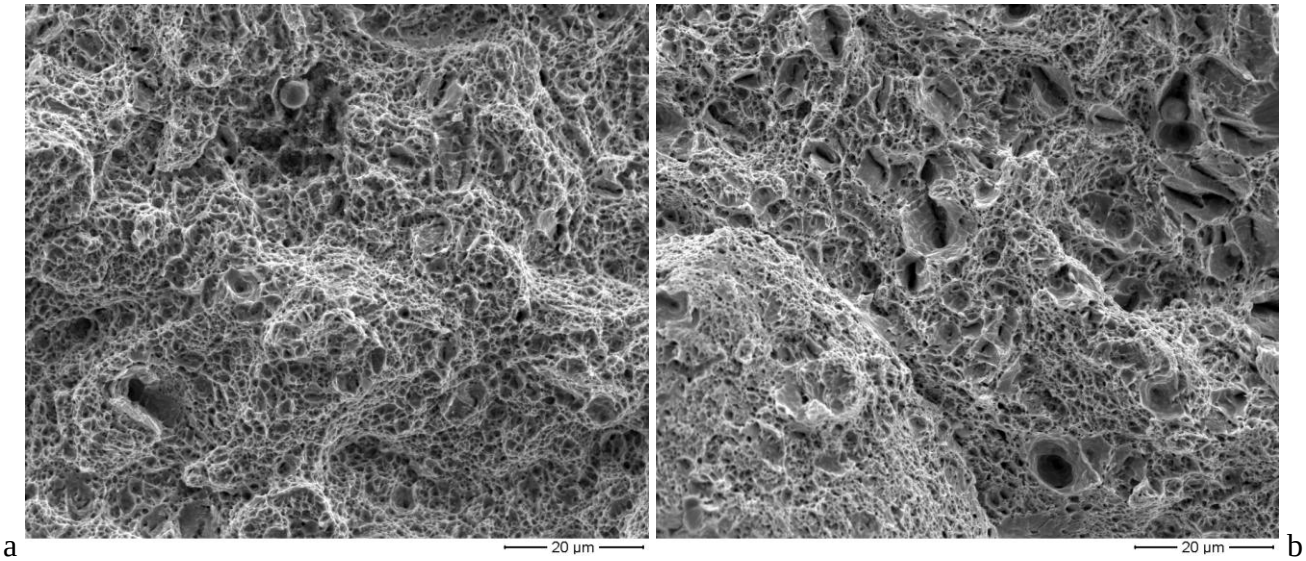

a b

Fig. 13 – Fracture surface of 39NiCrMo3 steel tensile specimens tempered at 320 °C (a) and 420 °C (b). Electron microscopy. Central (normal) part. Ductile fracture (a, b).

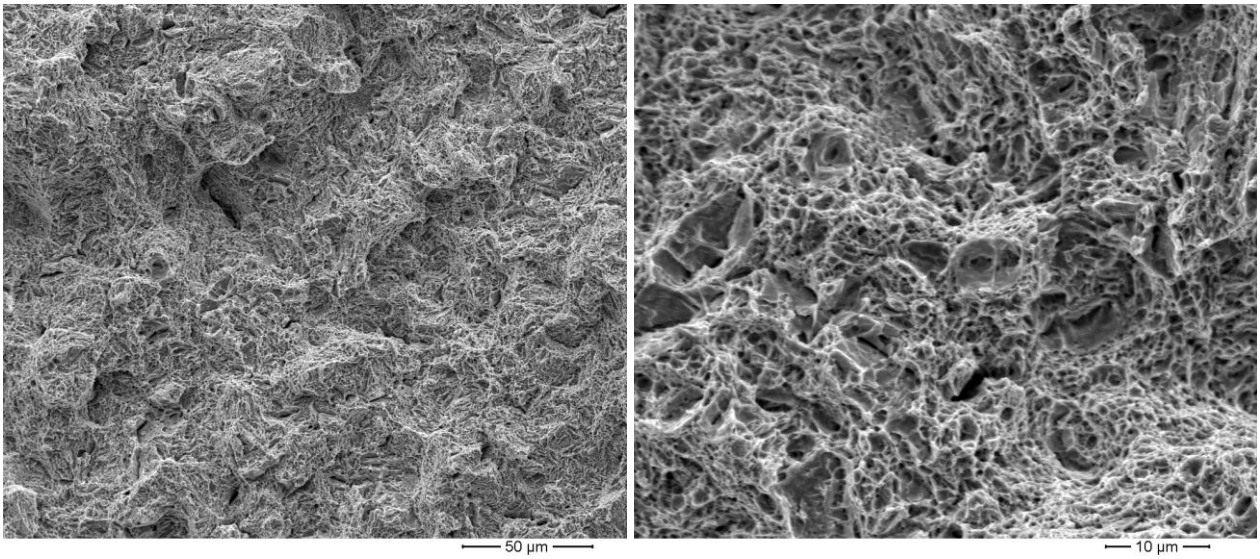

a b

Fig. 14 – Fracture surface of a 36NiCrMo16 steel tensile specimen tempered at 440 °C . Electron microscopy. Central (normal) part. Ductile fracture (a, b).

Table I - Elemental composition of the examined steel grades (mass %), optical emission spectroscopy.

Grade	C	Ni	Cr	Mo	Mn	Cu	Si	S	P	Al	V	Nb	B	Co	Ti
39NiCrMo3	0.42	0.87	0.75	0.18	0.70	0.08	0.22	0.009	0.013	0.015	0.006	0.001	0.0004	0.009	0.006
36NiCrMo16	0.36	3.7	1.7	0.28	0.53	0.49	0.29	0.012	0.012	0.026	0.011	0.005	0.0005	0.017	0.002